www.czasopisma.pan.pl PAN www.journals.pan.pl

Arch. Metall. Mater. **64** (2019), 3, 1183-1186

DOI: 10.24425/amm.2019.129511

JOONG-HWAN JUN*[#]

DEPENDENCE OF ROOM TEMPERATURE TENSILE PROPERTIES ON VOLUME FRACTION OF DISCONTINUOUS PRECIPITATES IN CAST AZ91 MAGNESIUM ALLOY

The objective of this study was to investigate the dependence of the room temperature tensile properties on the volume fraction of discontinuous precipitates (DPs) in a cast AZ91 magnesium alloy. In order to obtain various volume fractions of DPs, the solution-treated alloy was aged at 428 K for up to 48 h. The volume fraction of DPs increased from 0% to 72% with an increase in the aging time up to 24 h; for aging times longer than 24 h, discontinuous precipitation was substantially inhibited owing to the occurrence of significant continuous precipitation within the α-(Mg) grains. YS and UTS of the alloy increased with the volume fraction of DPs, whereas the elongation showed a reverse trend. A relatively rapid change in the tensile properties with increasing volume fraction of DPs up to ~40% was noted, which would be due to the reduction of the effective α grain size in response to the formation of DPs along the grain boundaries.

Keywords: discontinuous precipitates, microstructure, AZ91 alloy, aging, tensile properties

1. Introduction

Mg-Al-based alloys are the most commonly used Mg casting alloys on account of the beneficial combination of their mechanical properties at room temperature, die-castability, and corrosion resistance [1-4]. Mg-Al alloys with Al content higher than 6 wt% are generally age-hardened because of the large difference in the solid solubility of Al in Mg between the eutectic and ambient temperatures (12.9 wt% at 710 K and 2.9 wt% at 473 K, respectively) [5-7]. Precipitation of the $\beta(Mg_{17}Al_{12})$ phase from the supersaturated solid solution during aging treatment occurs either discontinuously or continuously, depending on the aging temperature [8-15]. Discontinuous precipitates (DPs) nucleate at grain boundaries and involve the cellular growth of alternating layers of the precipitate phase (β) and matrix phase (α), which eventually results in the formation of a lamellar structure behind a moving grain boundary [8-12]. Continuous precipitates (CPs) nucleate as isolated particles within the α-(Mg) grains and grow independently of other particles present in the grains [13,14]. Interestingly, the morphology of DPs in the Mg-Al alloy is identical to that of pearlite in steel, which is composed of alternating layers of the ferrite (bcc-Fe) and cementite (Fe_3C) phases [16-18].

The present study aims to investigate the effects of the volume fraction of DPs on the room temperature tensile properties of a cast AZ91 magnesium alloy. The relationship between the tensile properties and the volume fraction of DPs in the Mg-Al alloy needs to be examined in view of the fact that the mechanical properties of ferrite-pearlite steel are correlated to the volume fraction of pearlite [19-21].

2. Experimental procedures

The AZ91 alloy used in this study was prepared via melting commercial billet in a ($SF_6 + CO_2$) protective atmosphere and its subsequent casting into a steel mold. The chemical composition of the alloy was analyzed by inductively coupled plasma optical emission spectroscopy (ICP-OES; GBC Scientific Equipment Integra XM2) and determined as being Mg-8.6Al-0.9Zn-0.2Mn-0.003Fe-0.004Ni (wt%). Various specimens for microstructural observations and mechanical testing were prepared from the ingot via machining. In order to obtain various volume fractions of DPs, the specimens were solution-treated at 693 K for 24 h, water-quenched at room temperature, and then aged at 428 K for up to 48 h. The heat-treated specimens were mechanically polished, etched with a 5% Nital reagent, and then characterized by scanning electron microscopy (SEM; FEI Quanta 200). The volume fraction of DPs was measured by a point counting method. ASTM subsize specimens with a gauge length of 25 mm were used for the tensile tests, which were performed at room temperature on a versatile tensile testing machine (Instron 8802) at a crosshead speed of 1 mm/min.

* KOREA INSTITUTE OF INDUSTRIAL TECHNOLOGY, ADVANCED PROCESS AND MATERIALS R&D GROUP, INCHEON 21999, REPUBLIC OF KOREA

[#] Corresponding author: jhjun@kitech.re.kr

3. Results and discussion

Fig. 1 shows the change in the SEM microstructure of the AZ91 alloy with aging time at 428 K. In the as-solutionized state, the alloy is characterized by the α-(Mg) single phase with a trace amount of Al-Mn compound particles (Fig. 1a). As the aging time increases, nodules of DPs (white area) nucleate at the α-(Mg) grain boundaries and grow inside the grains. It is clearly observed from Fig. 1 that during aging at 428 K, the volume fraction of DPs increases consistently with an increase in the aging time up to 24 h. Blurred SEM images obtained after aging for 36 h and 48 h (Figs. 1e, 1f) may well be attributed to the occurrence of continuous precipitation within the remaining α-(Mg) matrix. Magnified SEM images of the AZ91 alloy aged for 12 h, 24 h, and 36 h are shown in Fig. 2. Discontinuous precipitation prevails after aging for 12 h (Fig. 2a), whereas fine CPs particles are observed within the α-(Mg) matrix region without DPs after 24 h of aging (Fig. 2b), even though their number density is negligibly small. After 36 h of aging, a mixed morphology consisting of DPs and high number density of CPs particles within the α-(Mg) matrix is evident in the microstructure (Fig. 2c). It is well established that discontinuous precipitation and continuous precipitation can occur simultaneously or competitively in Mg-Al alloys, depending on the aging temperature [8,9,11]. Discontinuous precipitation is dominant at low temperature, since the volume diffusion coefficient for continuous precipitation is approximately 6-7 orders of magnitude lower than the grain boundary diffusion coefficient for discontinuous precipitation [8]. Continuous precipitation tends to occur more favorably at high temperature owing to the increased bulk diffusivity, and both discontinuous precipitation and continuous precipitation can occur at intermediate temperatures [8]. The results shown in Figs. 1 and 2 imply that an aging temperature of 428 K is not low enough to completely suppress continuous precipitation in the AZ91 alloy. Therefore, continuous precipitation can occur at a later stage of aging, due to the slow kinetics of the nucleation and growth of CPs at this aging temperature.

Fig. 3 shows the change in the volume fraction of DPs in the AZ91 alloy with aging time at 428 K for up to 24 h. The volume fraction increases consistently with increasing aging

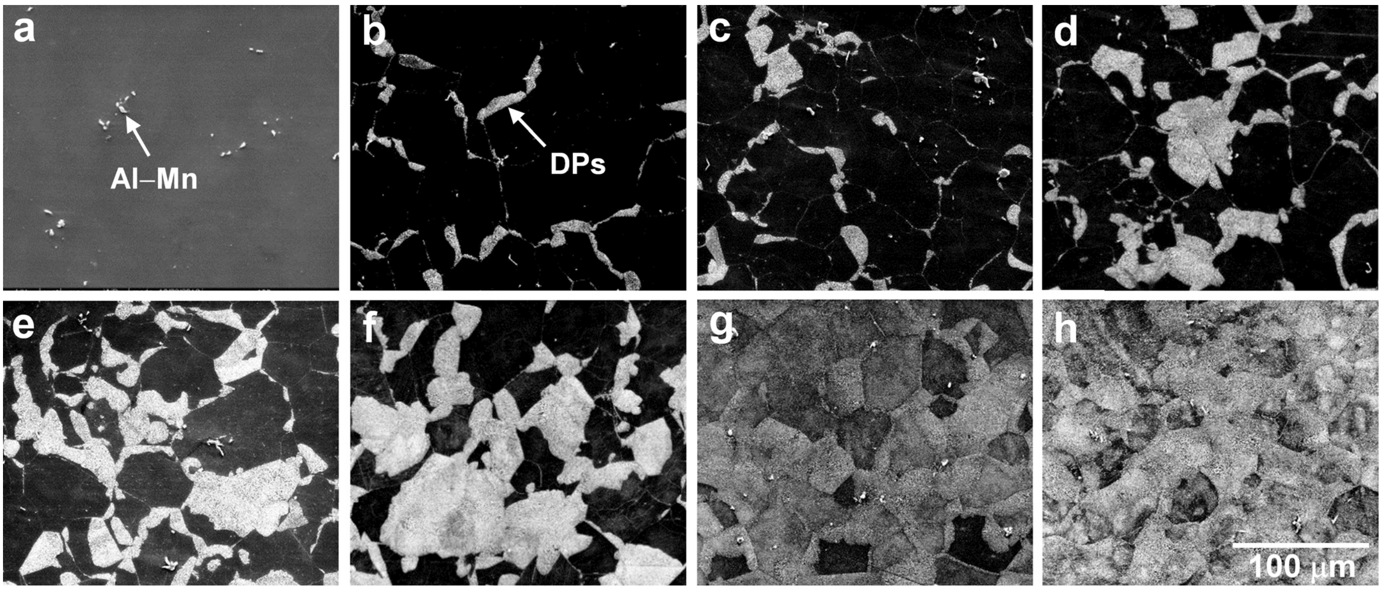

Fig. 1. SEM images of AZ91 alloy aged at 428 K for various times: (a) as-solutionized state, (b) 2 h, (c) 4 h, (d) 8 h, (e) 12 h, (f) 24 h, (g) 36 h, and (h) 48 h

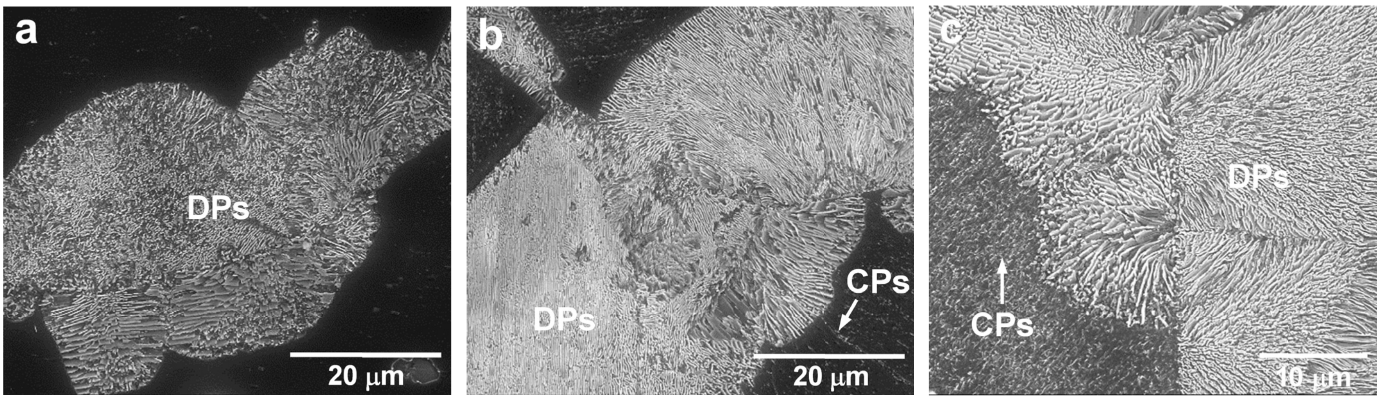

Fig. 2. Enlarged SEM images of AZ91 alloy aged at 428 K for (a) 12 h, (b) 24 h, and (c) 36 h

time up to 16 h, after which the formation of DPs becomes sluggish. The suppression of discontinuous precipitation at the later stage of aging is associated with the occurrence of CPs in the α-(Mg) matrix, as shown in Fig. 2. Continuous precipitation will reduce the supersaturation in the matrix ahead of the migrating discontinuous precipitation front, which will consequently reduce the driving force for discontinuous precipitation [8,9]. Moreover, continuous precipitation can play a role in pinning the migrating high-angle boundary necessary for the growth of DPs [9]. The volume fraction of DPs in the AZ91 alloy can vary in the range of 0%72% upon aging at 428 K up to 24 h before the onset of significant continuous precipitation. The change in the volume fraction of DPs with aging time was analyzed using the Johnson-Mehl equation [15], which is expressed as follows:

$$X = 1 - \exp(-(t/\tau)^n) \tag{1}$$

where X is the volume fraction of DPs, t is the aging time, τ is a time constant, and n is a coefficient characteristic of the transformation process. The plot of $\log\cdot\log(1/1-X)$ versus $\log t$ is shown in Fig. 4. The fitted data show a linear behavior, and the parameter n obtained from the slope of the line is equal to 1.09 for the AZ91 alloy. This value is very close to 1, which corresponds to the process of grain boundary nucleation after saturation [22].

Tensile tests of the AZ91 alloy with volume fractions of DPs up to 72% were conducted at room temperature; the test results are plotted in Fig. 5. The yield strength (YS) and ultimate tensile strength (UTS) of the alloy increased with the increase in the volume fraction of DPs up to 72%, whereas its elongation showed a reverse trend. This behavior can be easily explained by the increase in the volume fraction of harder and more brittle DPs in comparison to that of the α-(Mg) phase and is very similar to that of ferrite-pearlite steel, wherein the strengths and elongation exhibit increasing and decreasing tendencies, respectively, with increasing volume fraction of pearlite [19,20].

It is interesting to note that in Fig. 5, the tensile properties do not follow the linear law of mixtures and relatively steep changes in strengths and elongation with a change in the volume fraction of DPs up to ~40% are observed. According to the Zener-Hillert model [17], the interlamellar spacing (λ) of DPs can be expressed as:

$$\lambda = 4\gamma\cdot T_E/\Delta H_v\cdot\Delta T \tag{2}$$

where γ is the surface energy of the α/β interface, T_E is the eutectic temperature, ΔH_v is the change in enthalpy between the α and β phases, and ΔT is the degree of undercooling. Given that γ and ΔH_v are relatively independent of temperature and that the DPs of the AZ91 alloy were formed by isothermal aging at 428 K in this work, the λ values of the DPs are almost identical regardless of the aging time. This indicates that the strength and strain values of the DPs are unlikely to change with the volume fraction of DPs in the AZ91 alloy. In view of the fact that DPs form along the grain boundaries and grow inside the α-(Mg) grains, as observed in Fig. 1, the increase in the volume fraction of DPs can lead to a reduction of the effective grain size of the

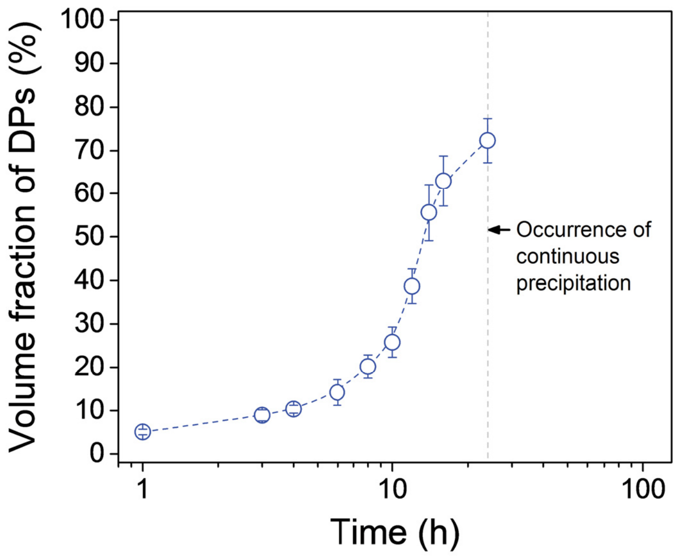

Fig. 3. Change in volume fraction of DPs with aging time at 428 K in AZ91 alloy

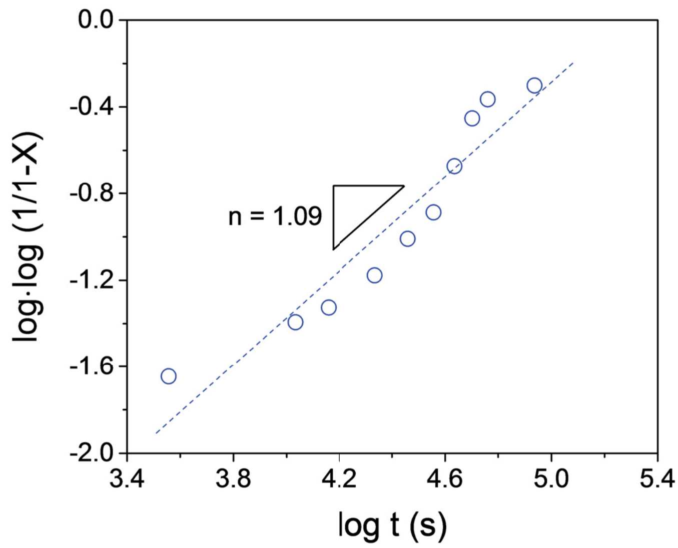

Fig. 4. Change in $\log\cdot\log(1/1-X)$ with $\log t$ at 428 K in AZ91 alloy

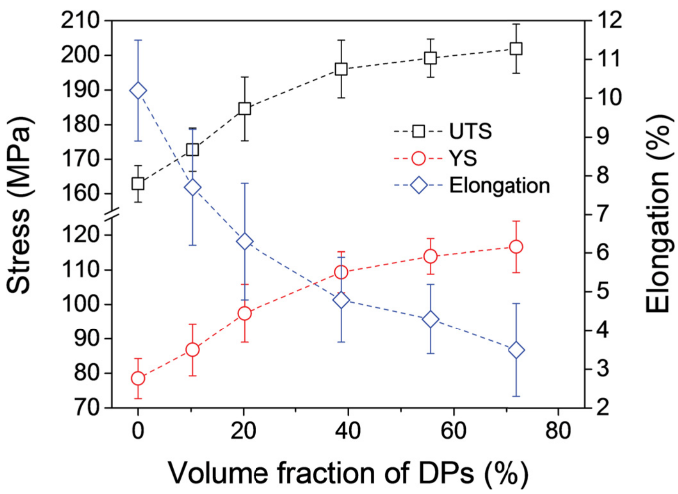

Fig. 5. Changes in YS, UTS, and elongation with volume fraction of DPs in AZ91 alloy

α-(Mg) phase, by which the strength and strain values of the α-(Mg) actually show increasing and decreasing trends, respectively, with increasing the volume fraction of DPs. Consequently, the rapid change in the tensile properties with volume fraction of DPs up to ~40% can be explained by the increase and decrease in strength and strain values of the α-(Mg) phase, respectively. The refining effect of the α-(Mg) grains on the strength and strain values of the α-(Mg) phase will become weaker when a greater part of the microstructure is occupied by DPs.

4. Conclusions

The purpose of this study was to investigate the dependence of the room temperature tensile properties on the volume fraction of DPs in the cast AZ91 magnesium alloy. In order to obtain various volume fractions of DPs, the solution-treated alloy was aged at 428 K for up to 48 h. The volume fraction of DPs increased from 0% to 72% with an increase in the aging time up to 24 h; for aging times longer than 24 h, discontinuous precipitation was substantially inhibited owing to the occurrence of significant continuous precipitation. The YS and UTS of the alloy increased with increasing volume fraction of DPs, whereas its elongation showed a reverse trend. It was noted that the change in the tensile properties was relatively rapid up to a DPs volume fraction of ~40%. This change is thought to be related to the reduction of the effective grain size of the α-(Mg) phase caused by the formation of DPs along the grain boundaries and their growth inside the grains.

Acknowledgement

This study was supported by the Korea Institute of Industrial Technology (KITECH UR-18-0014).

REFERENCES

[1] A.K. Dahle, Y.C. Lee, M.D. Nave, P.L. Schaffer, D.H. StJohn, J. Light Met. **1**, 61 (2001).
[2] B.L. Mordike, T. Ebert: Mater. Sci. Eng. A **302**, 37 (2001).
[3] H. Cao, M. Wessén, Metall. Mater. Trans. A **35A**, 309 (2004).
[4] G. Song, A. Atrens, Adv. Eng. Mater. **9**, 177 (2007).
[5] S. Celotto, T.J. Bastow, Acta Mater. **49**, 41 (2001).
[6] H. Okamoto, Desk Handbook Phase Diagrams for Binary Alloys, ASM International, Ohio (2000).
[7] C.R. Hutchinson, J.F. Nie, S. Gorsse, Metall. Mater. Trans. A **36A**, 2093 (2005).
[8] K.N. Braszczyńska-Malik, J. Alloys Compd. 477, 870 (2009).
[9] J.D. Robson, Acta Mater. **61**, 7781 (2013).
[10] E.A. Brener, D.E. Temkin, Acta Mater. **51**, 797 (2003).
[11] D. Duly, J.P. Simon, Y. Brechet, Acta Metall. Mater. **43**, 101 (1995).
[12] D. Duly, Y. Brechet, Acta Metall. Mater. **42**, 3035 (1994).
[13] S. Celotto, Acta Mater. **48**, 1775 (2000).
[14] M.X. Zhang, P.M. Kelly, Scr. Mater. **48**, 647 (2003).
[15] D. Duly, Y. Brechet, B. Chenal, Acta Metall. Mater. **40**, 2289 (1992).
[16] K.K. Ray, D. Mondal, Acta Metall. Mater. **39**, 2201 (1991).
[17] N. Ridley, Metall. Trans. A **15A**, 1019 (1984).
[18] E.M. Taleff, J.J. Jewandowski, B. Pourladian, JOM **54**, 25 (2002).
[19] R. Mizuno, H. Matsuda, Y. Funakawa, Y. Tanaka, Tetsu-to-Hagané **96**, 414 (2010).
[20] L.I. Gladshtein, N.P. Larionova, B.F. Belyaev, Metallurgist **56**, 579 (2012).
[21] L. Wang, D. Tang, Y. Song, J. Iron Steel Res. Int. **24**, 321 (2017).
[22] D. Bradai, M. Kadi-Hanifi, P. Zieba, W.M. Kuschke, W. Gust, J. Mater. Sci. **34**, 5331 (1999).